

Adjustment of gripping force by optical systems

C K Jalba and C Barz

Technical University Cluj Napoca, North University Center Baia Mare, Str. Doctor Victor Babeş 62A, Baia Mare 430083, Romania

E-mail: klausjalba@t-online.de

Abstract. With increasing automation, robotics also requires ever more intelligent solutions in the handling of various tasks. In this context, many grippers must also be re-designed. For this, they must always be adapted for different requirements. The equipment of the gripper systems with sensors should help to make the gripping process more intelligent. In order to achieve such objectives, optical systems can also be used. This work analyzes how the gripping force can be adjusted by means of an optical recognition. The result of this work is the creation of a connection between optical recognition, tolerances, gripping force and real-time control. In this way, algorithms can be created, with the aid of which robot grippers as well as other gripping systems become more intelligent.

1. Introduction

In today's gripping technology, the grippers are increasingly specialized in specific gripping procedures.

In a gripping operation are involved various physical parameters, for example the gripping force, the weight of the gripped object, the friction between the gripper jaws and the gripped object, torques, etc. Regardless of the size of these forces there is a link between the distances between the gripper jaws and the object to be gripped.

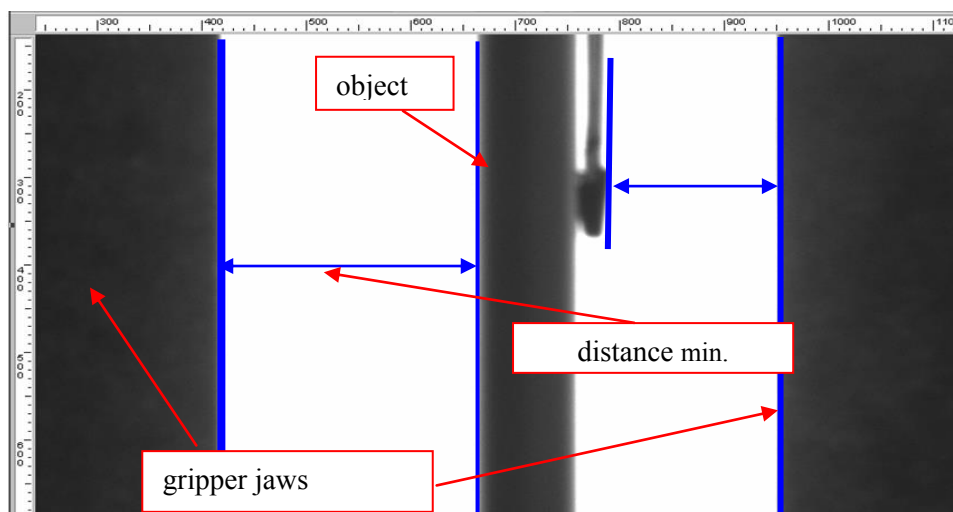


Figure 1. Magnification 5.5x



These distances tend to be zero, but they certainly do not reach this limit. For this reason, were made attempts to find out how these infinitesimal distances could be quantified. In the next two figures can be seen the same picture, by an enlargement of 550% (Figure 1) and 2500% (Figure 2).

In the first case, the contours from the object seems to be a clear well-defined line. But in the second picture it can be seen, that the contour is in fact a line with undefined accounts. The object contour becomes an optical field within certain boundaries. These boundaries can be viewed as a tolerance field.

A promising approach to measure this tolerance field was to make measurements in the tolerance system used in the mechanical engineering. In this system, the fits are divided into three categories: the clearance fit, the transition fit, and the press fit. If the tolerance is too great, the object falls between the fingers of the gripper, if it is too tight, then a softer object can be crushed.

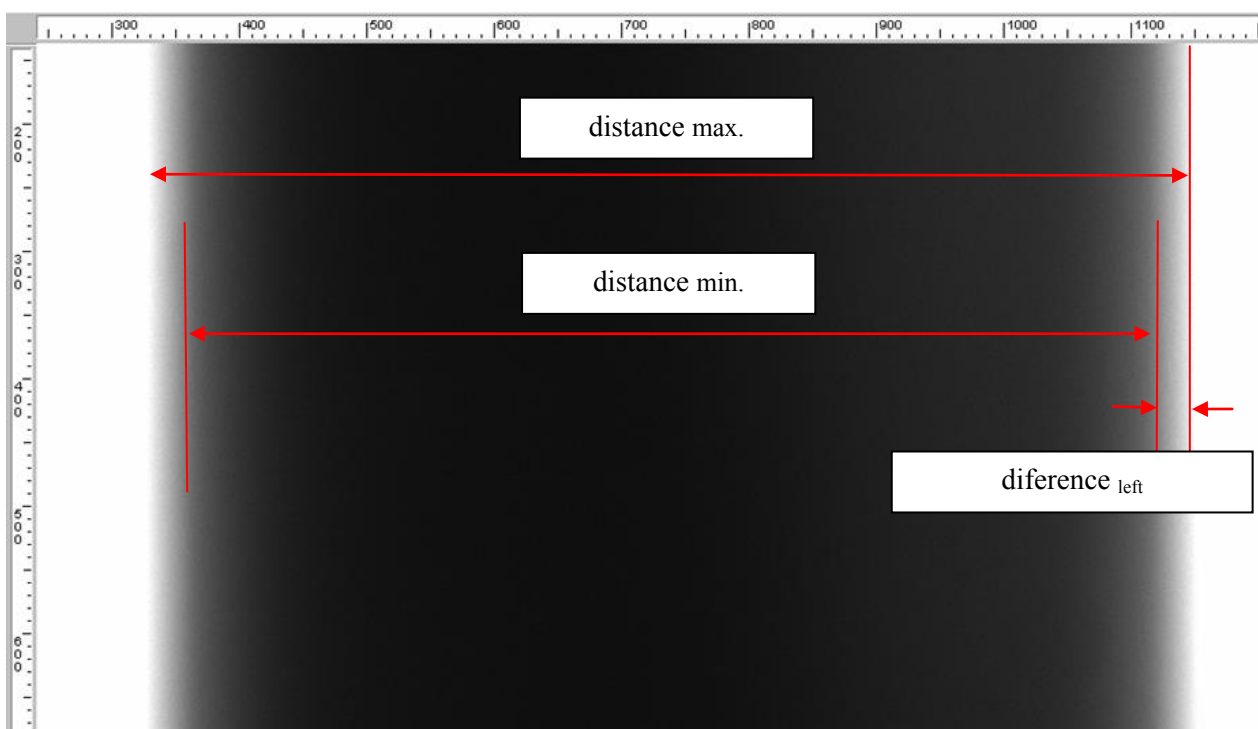


Figure 2. Magnification 20x

Only in the case of transitional adjustment does it seem that the objects are not falling through the jaws of the gripper, nor are they squeezed by excessive forces.

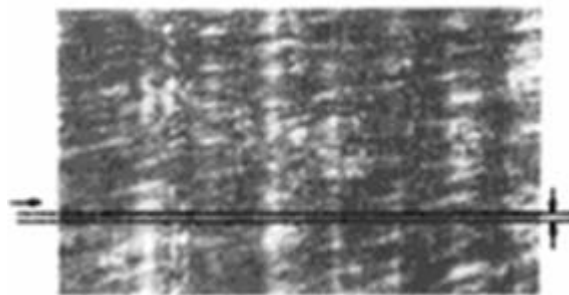


Figure 3. Metallic surface [1]

Because the tolerances of the transition fit are known from tables and they are located in the range of less than one millimeter, a measuring method must be found that can detect these tolerances. A method to find out this kind of tolerances is for example the measurement of material surfaces with roughness testers.

Figure 3 shows a metal surface machined by cutting. In the section, the surface of the metallic object has micron scattering (Figure 4) [1], [2].

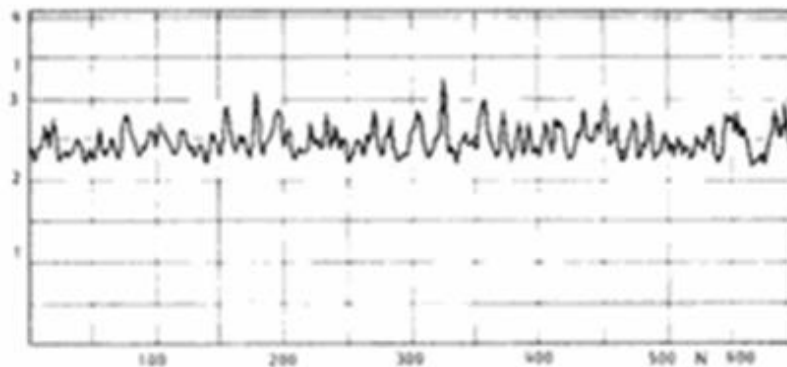


Figure 4. Section of a metallic surface [2]

Measurements with roughness testers are usually made with devices, which analyze surfaces with different mechanical sensors. The head with the touch sensor (Figure 6) slides on an air bed to avoid friction between the sensor and the object. Thus, the system becomes very sensitive and can measure by touching surfaces with accuracy of the order of the hundredth of mm (Figure 5). The whole assembly is positioned on a heavy polished granite plate. This plate gives a considerable inertia to the measurement system, being adapted to the dynamic forces of the translational movements [3].

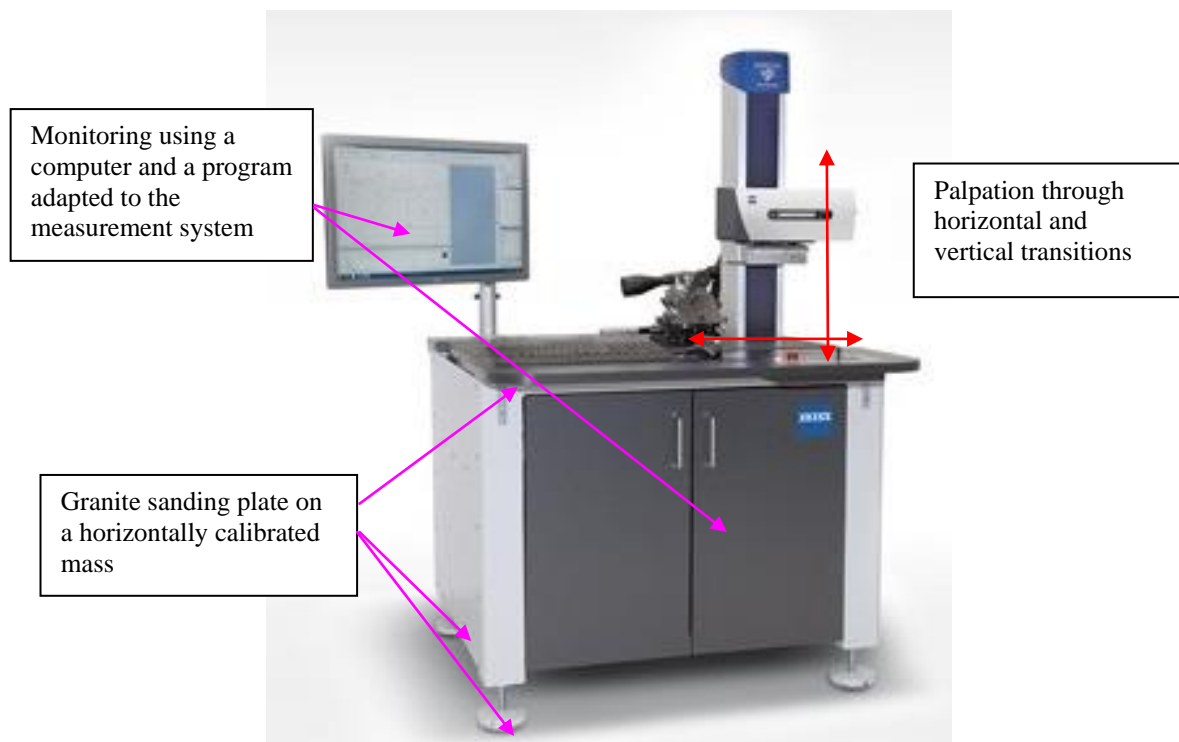


Figure 5. Roughness measurement with ZEISS SURFCOM [3]

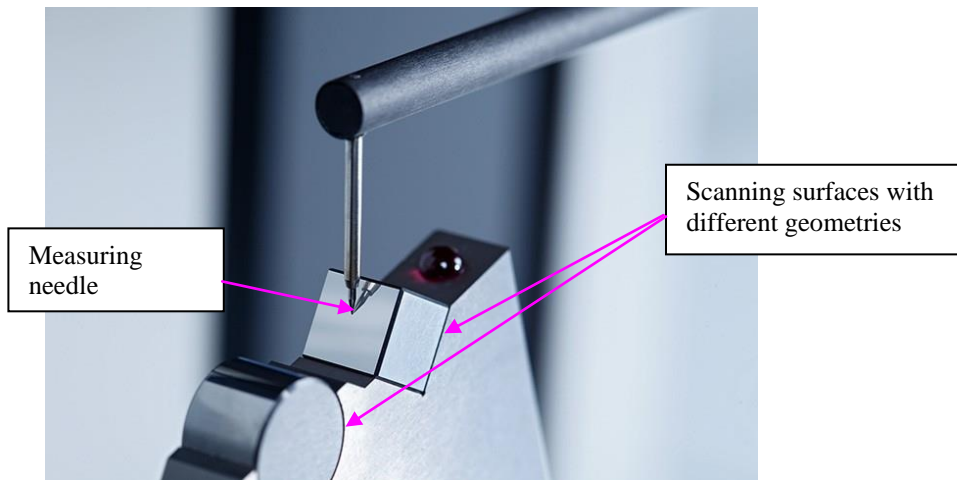


Figure 6. Section of a metallic surface [2]

For our measurements was used a ZEISS SURFCOM 1900 SD device (Figure 6) to pin out contours and asperities. The system can be equipped with tactile sensors as well as optical sensors. This system can reach a resolution of 0.016 mm with maximum sensitivity of 2 μm , 5 μm or 10 μm depending on the measuring head used (Figure 7).

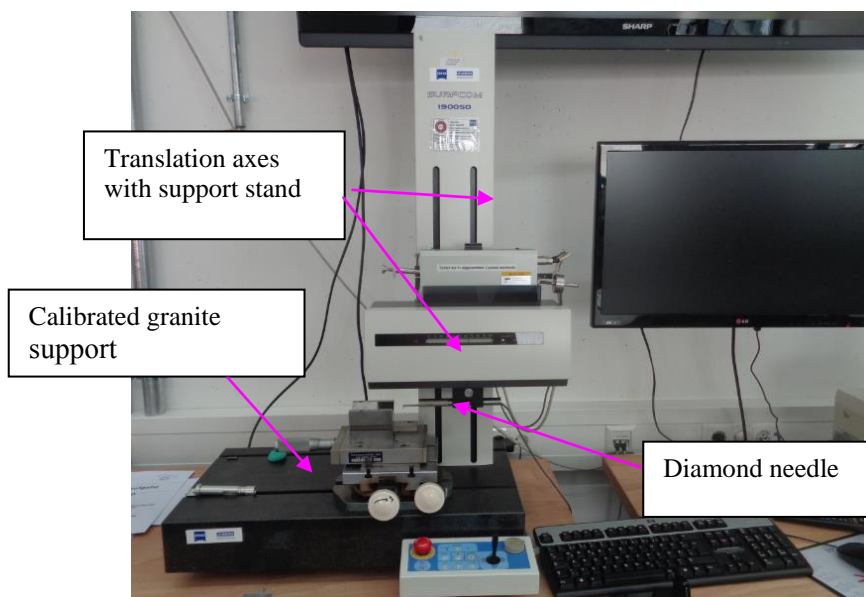


Figure 7. Workplace with ZEISS SURFCOM 1900 SD

With this system, measurements can be made for very fine rays, angles, phases or finishes, as measuring devices can be adapted to the requirements by changing the measuring heads. The possible track of measurement is 100 or 200 mm long.

2. Mathematical modeling

In the following example was measured the surface of a S235 steel shaft. In the graph (Figure 8) can be seen the roughness of the chipping process. The image was magnified vertically 2,000 times and horizontally 30.43 times.

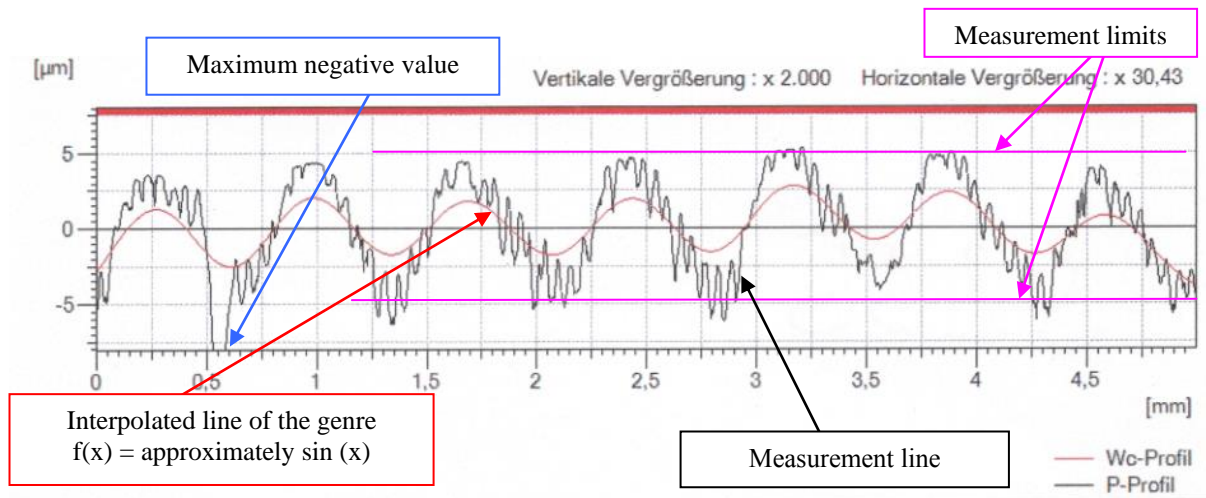


Figure 8. Roghness

According to this chart, the following values were obtained:

- Ra = 1,7043 μm (average asperity)
- Rz = 8,0779 μm (the average depth of asperities)
- Rzmax = 12,1734 μm (maximum depth of asperity)
- RSm = 275,0469 μm (average length of asperities)

The average of monitored asperities can then be considered as a function approximate to the formula $f(x) = (\sin x)$. This line does not show the exact asperities resulting from the cutting of the shaft, but in certain tolerances in the range of microns, can indicate the path traveled by the measuring head. In this way, extreme values can be eliminated and the trend of the function $f(x)$ is visualized (Figure 9). For the above example, by mathematical modeling, the following function can be obtained for the entire interval: $y = f(x)$

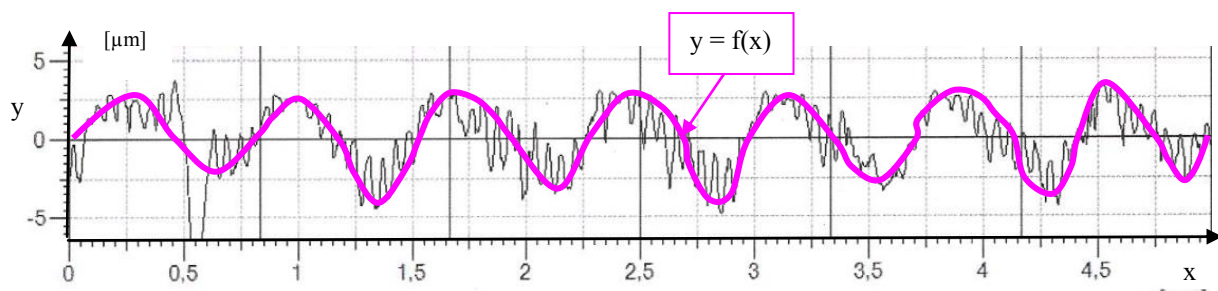


Figure 9. The trend of function $f(x)$

where

$$f(x) = f(x_1) + f(x_2) + f(x_3) + f(x_4) + f(x_5) + f(x_6) = \sum_1^6 f(x) \tag{1}$$

and generally

$$f(x) = f(x_1) + \dots + f(x_n) = \sum_{i=1}^n f(x) \tag{2}$$

By mathematical iteration, applying for example the Newton approximation, the function obtained is: $f(x) = 3\sin(7,5x)$

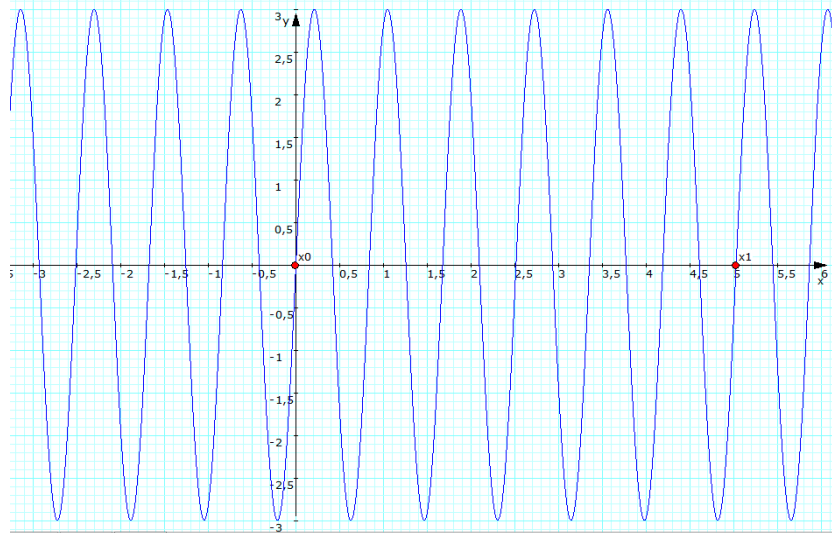


Figure 10. Approximate function

with the following values obtained by iteration (Table 1):

Table 1. Iteration resultes

| Points | Bisection | Falsi Rule | Newton |
|--------|----------------------|------------------------|-----------------------|
| P 1 | (-1 -3,458589) | (-1 -3,458589) | (-1 -3,458589) |
| P 2 | (2 1,060914) | (2,475096 0,725091) | (-0,163263 -3,386907) |
| P 3 | (0,5 -2,277188) | (1,872812 3,360299) | (0,237104 3,386907) |
| P 4 | (1,25 -0,696104) | (0,457111 -1,292247) | (0,735508 -2,032976) |
| P 5 | (1,625 -0,188456) | (1,326294 -2,480521) | (0,828179 0,327795) |
| P 6 | (1,8125 3,442877) | (7,226111 -2,758128) | (0,815962 -0,000966) |
| P 7 | (1,71875 2,167972) | (39,617143 -1,092724) | (0,815998 0) |
| P 8 | (1,671875 1,057924) | (58,377015 -0,883749) | |
| P 9 | (1,648438 0,441911) | (78,756683 -0,346201) | |
| P 10 | (1,636719 0,127245) | (87,628283 2,267156) | |
| P 11 | (1,630859 -0,030637) | (52,535186 2,371658) | |
| P 12 | (1,633789 0,048317) | (30,757866 -3,282152) | |
| P 13 | (1,632324 0,008841) | (621,530912 -3,183733) | |
| | | | |
| P 23 | (1,631997 0,000012) | | |
| P 24 | (1,631996 -0,000007) | | |
| P 25 | (1,631996 0,000002) | | |
| P 26 | (0,631996 -0,00002) | | |
| P 27 | (0,631996 0) | | |

If the function graph $f(x) = 3\sin(7.5x)$ is adjusted by scaling and expansion to the graph of the ZEISS SURFCOM 1900 SD (figure), then these two graphs become almost identical (Figure 11).

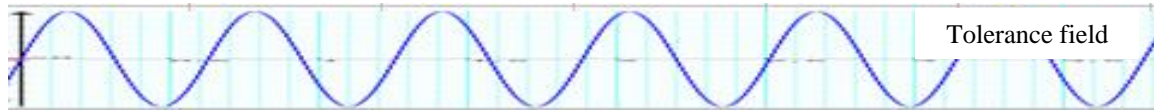


Figure 11. Adapted function graph

To compare mathematically the surface of the graph with surfaces obtained by other measuring methods, these surfaces are to be integrated according to the formula:

$$f(x) = \int 3\sin(7,5x)dx = \int 3\sin\left(\frac{15}{2}\right)xdx \rightarrow F(x) = -\frac{2\cos\left(\frac{15x}{2}\right)}{5} + C \quad (3)$$

According to the ZEISS SURFCOM 1900 SD monitoring system presented in this paper, there were also used for optoelectronic measurements, [4-6] where the tolerance field had to be around 10 μm , an industrial processing system. The system has a camera, a lighting plate, an adjustable tripod and an image processing program (Figure 12).

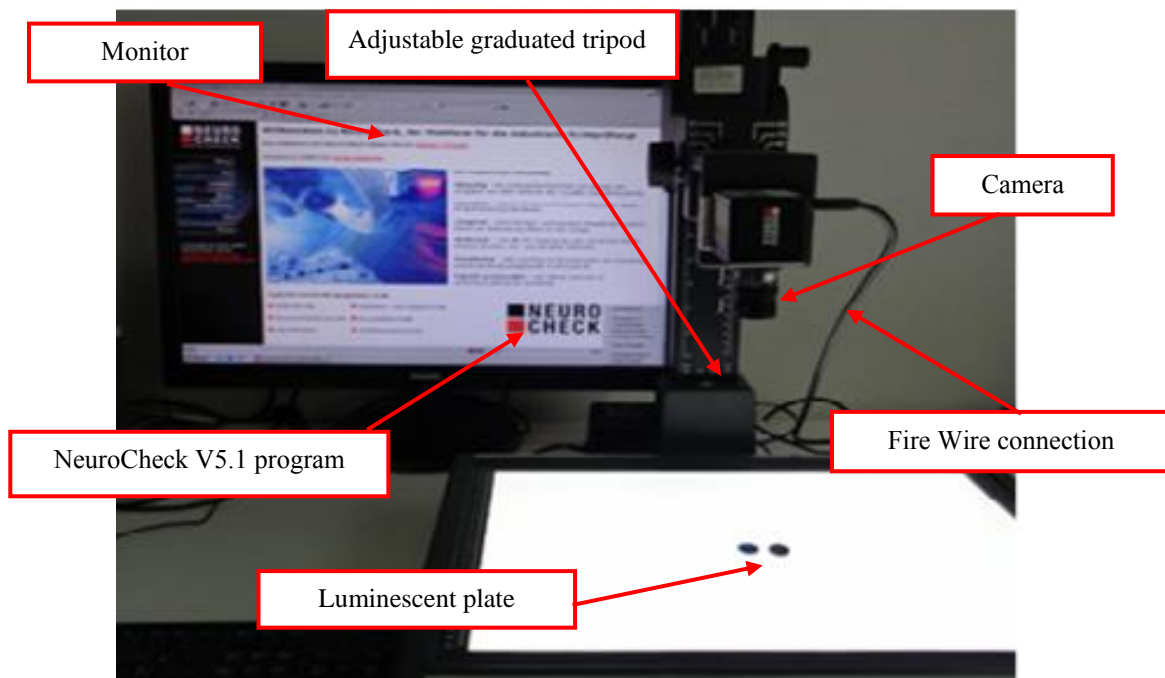


Figure 12. Work place for image recognition [6]

The data obtained from several series of simulations with objects of different shapes and sizes gave results similar to those obtained with the ZEISS measurement system. In the following figure can be seen the tolerances from the measurement of an object and in which tolerance field the measurements were framed (Figure 13).

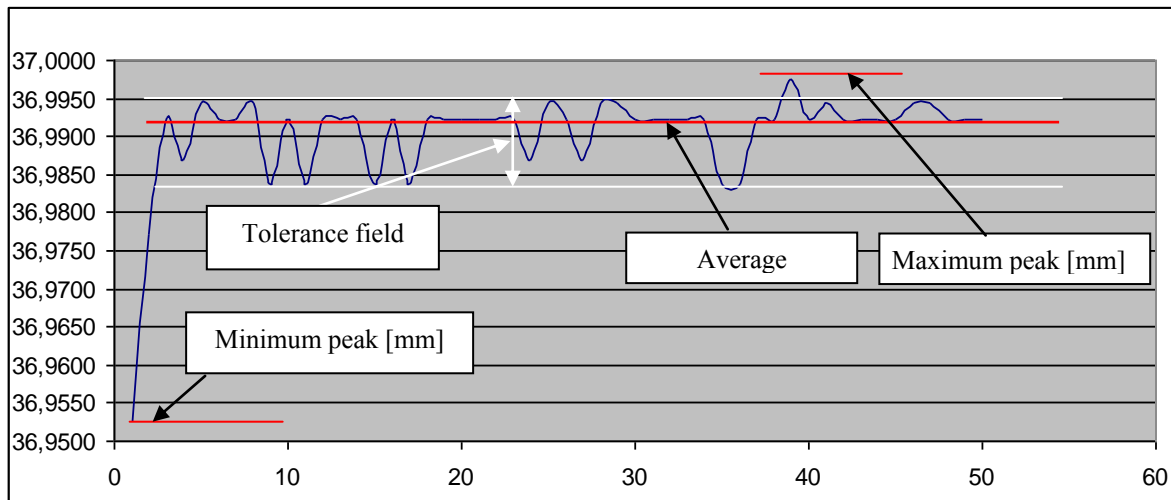


Figure 13. Measurements with image recognition

The measurements offered a series of representative results, from which the following information was extracted:

- The arithmetic means of the string according to the formula:

$$\bar{x} = \frac{1}{n}(x_1 + x_2 + x_3 + \dots + x_n) = \frac{1}{n} \sum_{i=1}^n x_i \quad (4)$$

where - \bar{x} is the arithmetic mean,

x_i is an element of the string,

n is the number of the elements in the string,

with

$$\Delta x = \sigma_n \quad (5)$$

where: - Δx is the deviation for a single measurement,

- The variance according to the formula:

$$s^2 = \frac{1}{n-1} [(x_1 - \bar{x})^2 + (x_2 - \bar{x})^2 + \dots + (x_n - \bar{x})^2] = \frac{1}{n-1} \sum_{i=1}^n (x_i - \bar{x})^2 \quad (6)$$

- The standard deviation according to the formula:

$$\sigma_n = \sqrt{\frac{1}{n-1} \sum_{i=1}^n (x_i - \bar{x})^2} \quad (7)$$

where: - σ_n is the standard deviation,

$$\Delta \bar{x} = \frac{\sigma_n}{\sqrt{n}} \quad (8)$$

where: - $\Delta \bar{x}$ is the deviation from the arithmetic mean,

- The median, the value that divides the ordered statistical series into two equal subsets, the volumes being measured in the number of statistical units according to the formulas:

$$n = 2 p + 1 \quad (9)$$

If the series has an odd number of values and

$$n = 2 p \quad (10)$$

If the series has a just number of values,

- The variance coefficient v according to the formula:

$$v = \frac{s}{x} \cdot 100 \quad (11)$$

- Maximum deviations,

- Minimum deviations.

The results of this measurement can be seen in the following table (Table 2).

Table 2. Measuremets results

| Temperature | 23°C | 4°C |
|------------------------|------------|-------------|
| Diameter max. [mm] | 40.5064 | 40.4569 |
| Diameter min. [mm] | 40.4816 | 40.4242 |
| Total | 4049.1215 | 4044.3711 |
| Math. average [mm] | 40.491215 | 40.443711 |
| Number of attempts n | 100 | 100 |
| Standard deviation | 0.00901976 | 0.007228581 |
| Median [mm] | 40.4876 | 40.4433 |
| Variance | 8.1356E-05 | 5.22524E-05 |
| Variance coefficient % | 2.22758395 | 1.78731626 |

According to data obtained from the measurements we have chosen for (Figure 14), [7], [8]

- upper tolerance ES = 0.004 mm (for 0.0064 mm)

- lower tolerance EI = -0,016 mm (for 0,0284 mm).

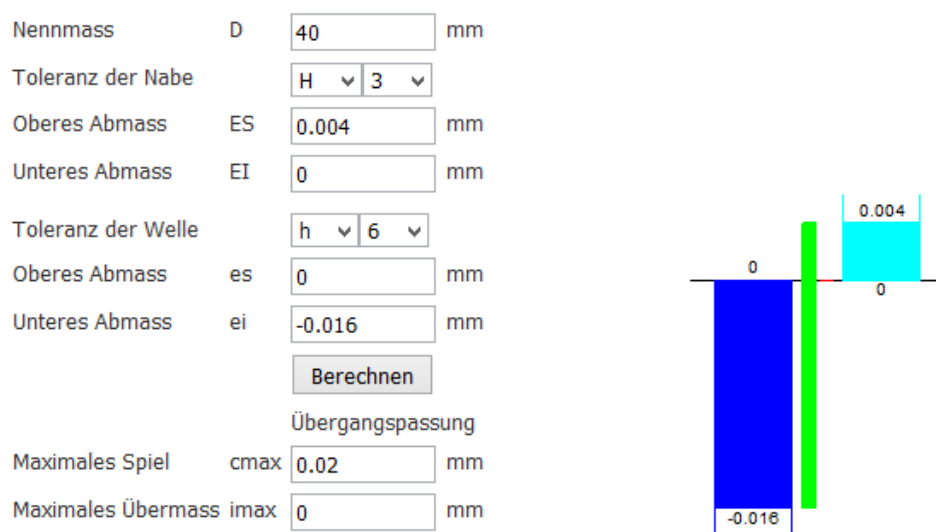


Figure 14. Calculation in Adjustment System [7]

These tolerances result in a combination of the H3 / h6 form, which means that the result of the measurements falls within the intermediate adjustment system (Figure 14).

3. Conclusions

As such, it has been shown that the resolution of the image recognition system is sufficiently precise for a smart intelligent gripping system to catch and pick up fragile objects without additional pressure sensors.

Numerical simulations helped determine contours resulting from surfaces. The results thus obtained can be processed in the algorithms for step-by-step motors programming for the exact operation of the gripper, respectively for the operation of the industrial robots used in the gripping process.

References

- [1] Ahlers R J 1986 *Die Optische Rauheitsmessung in der Qualitätstechnik*, Springer-Verlag Berlin Heidelberg
- [2] Burkhardt T, Feinäugle A, Fericean S and Forkl A 2004 *Lineare Weg- und Abstandssensoren: Berührungslose Messsysteme für den industriellen Einsatz*, Neuhausen
- [3] ***2017 ZEISS SURFCOM, Carl Zeiss AG, internet site called 15.06.2017 <https://www.zeiss.com/metrology/products/systems/form-and-surface/cnc-surface-measuring-instruments/surfc0m-1500.html>
- [4] Demant C, Streicher-Abel B and Waszkewitz P 2011 *Industrielle Bildverarbeitung*, Third Edition, Springer-Verlag Berlin Heidelberg, New York
- [5] Gonzalez R C and Woods R E 1992 *Digital Image Processing*, Addison-Wesley, Reading MA
- [6] Jalba C K, Muminovic A, Epple S, Nasui V and Barz C 2016 Optical Gripper, *IOP Conf. Ser.: Mater. Sci. Eng.* **200** 012054
- [7] ***2017 MESYS AG, Technoparkstrasse 1, 8005 Zürich, internet site called 20.03.2017 <https://www.mesys.ch/?cat=5>
- [8] Schweizer A 2016 *Formelsammlung und Berechnungsprogramme für Anlagenbau*, Wasenöschstr. 11, DE 88048 Friedrichshafen